

Synthesis and Characterization of Stable Ruthenabenzenes Starting from HC≡CCH(OH)C≡CH

Hong Zhang, Li Feng, Lei Gong, Liqiong Wu, Guomei He, Tingbin Wen, Fangzu Yang, and Haiping Xia*

College of Chemistry and Chemical Engineering, State Key Laboratory for Physical Chemistry of Solid Surfaces, Xiamen University, Xiamen, 361005, People's Republic of China

Received March 2, 2007

Treatment of RuCl₂(PPh₃)₃ with HC≡CCH(OH)C≡CH/PPh₃ at room temperature produces the air-stable ruthenabenzene [Ru(CHC(PPh₃)CHC(PPh₃)CH)Cl₂(PPh₃)₂]Cl (**2**) in good yield. The ruthenabenzene **2** can even be obtained from the one-pot reaction of RuCl₃, PPh₃, and HC≡CCH(OH)C≡CH in the mixed solvent of ionic liquid and CH₂Cl₂ in higher yield. The ruthenabenzene **2** reacts with PMe₃, PBu₃, *tert*-butyl isocyanide, 2,2'-dipyridyl (bipy), and 2,2'-dipyridyl/PMe₃ to give new stable ruthenabenzene [Ru(CHC(PPh₃)CHC(PPh₃)CH)Cl₂(PMe₃)₂]Cl (**4**), [Ru(CHC(PPh₃)CHC(PPh₃)CH)Cl₂(PBu₃)₂]Cl (**5**), [Ru(CHC(PPh₃)CHC(PPh₃)CH)Cl(BuNC)(PPh₃)₂]Cl₂ (**6**), [Ru(CHC(PPh₃)CHC(PPh₃)CH)Cl(bipy)(PPh₃)Cl₂ (**7**), and [Ru(CHC(PPh₃)CHC(PPh₃)CH)(bipy)(PMe₃)₂]Cl₃ (**8**), respectively. Reaction of ruthenabenzene **2** with AgBF₄ gives bisruthenabenzene [Ru(CHC(PPh₃)CHC(PPh₃)CH)(PPh₃)₂](μ-Cl)₃(BF₄)₃ (**9**). The thermal decomposition reactions of ruthenabenzene **2** and **7** produce a stable Cp⁻ ion derivative, [CHC(PPh₃)CHC(PPh₃)CH]Cl (**10**). **2**, **4**, **7**, **8**, **9**, and **10** have been structurally characterized. **9** is the first non-metal-coordinated bismetallabenzene. An electrochemical study shows that the metal centers in the bisruthenabenzene **9** slightly interact with each other through the chloro bridges.

Introduction

The chemistry of transition metal-containing metallabenzene¹ is attracting considerable current attention both experimentally² and theoretically.³ Metallabenzene are interesting because they can display aromatic properties and they can mediate organometallic reactions. One of the major issues of metallabenzene chemistry is the isolation and characterization of stable metallabenzene. The first stable transition metal-containing met-

allabenzene was reported in 1982 by Roper et al.⁴ Since then, a number of stable metallabenzene have been successfully isolated and characterized. Most of the well-characterized stable metallabenzene are those with a transition metal of the third transition series, especially osmium,^{2b,4–7} iridium,^{2c–f,h,i,8} and platinum.^{2g,j} In contrast, well-characterized metallabenzene with a metal of the first and the second transition series are still very rare, although the possibility of isolation of such species has been predicted theoretically as early as 1979.¹⁰ While coordinated metallabenzene with a metal of the first¹¹ and the second^{12,13} transition series and 1,3-dimetallabenzene¹⁴ of Nb and Ta have been isolated and well characterized, isolation of free metallabenzene with a metal of the first and the second transition series has met with limited success. The ruthenabenzene CpRu(C(Ph)CHCHC(Ph)C(OEt))(CO) and related ruthenaphenoxide and ruthenaphenanthrene oxide reported by Jones and Allison represent rare examples (and the only reported examples, to the best of our knowledge) of spectroscopically characterized metallabenzene with a metal of the second transition series.^{15a} However, these species are thermally unstable at ambient temperature. Other metallabenzene such as ferrobenezene,^{16a} ruthenaphenanthrene,^{15a} ruthenaphenol,^{15b}

* Corresponding author. Fax: (+86)592-218-6628. E-mail: hpxia@xmu.edu.cn.

(1) (a) Wright, L. J. *Dalton Trans.* **2006**, 1821. (b) Landorf, C. W.; Haley, M. M. *Angew. Chem., Int. Ed.* **2006**, *45*, 3914. (c) Jia, G. *Acc. Chem. Res.* **2004**, *37*, 479. (d) Bleeke, J. R. *Chem. Rev.* **2001**, *101*, 1205.

(2) Examples of recent experimental work: (a) Hung, W. Y.; Zhu, J.; Wen, T. B.; Yu, K. P.; Sung, H. H. Y.; Williams, I. D.; Lin, Z.; Jia, G. *J. Am. Chem. Soc.* **2006**, *128*, 13742. (b) Clark, G. R.; Johns, P. M.; Roper, W. R.; Wright, L. J. *Organometallics* **2006**, *25*, 1771. (c) Alvarez, E.; Paneque, M.; Poveda, M. L.; Rendon, N. *Angew. Chem., Int. Ed.* **2006**, *45*, 474. (d) Wu, H. P.; Weakley, T. J. R.; Haley, M. M. *Chem.–Eur. J.* **2005**, *11*, 1191. (e) Chin, C. S.; Lee, H.; Eum, M. S. *Organometallics* **2005**, *24*, 4849. (f) Chin, C. S.; Lee, H. *Chem.–Eur. J.* **2004**, *10*, 4518. (g) Landorf, C. W.; Jacob, V.; Weakley, T. J. R.; Haley, M. M. *Organometallics* **2004**, *23*, 1174. (h) Gilbertson, R. D.; Lau, T. L. S.; Lanza, S.; Wu, H. P.; Weakley, T. J. R.; Haley, M. M. *Organometallics* **2003**, *22*, 3279. (i) Paneque, M.; Posadas, C. M.; Poveda, M. L.; Rendón, N.; Salazar, V.; Oñate, E.; Mereiter, K. *J. Am. Chem. Soc.* **2003**, *125*, 9898. (j) Jacob, V.; Weakley, T. J. R.; Haley, M. M. *Angew. Chem., Int. Ed.* **2002**, *41*, 3470. (k) Bleeke, J. R.; Hinkle, P. V.; Rath, N. P. *Organometallics* **2001**, *20*, 1939. (l) Bleeke, J. R.; Blanchard, J. M. B.; Donnay, E. *Organometallics* **2001**, *20*, 324. (m) Hughes, R. P.; Trujillo, H. A.; Egan Jr., J. W.; Rheingold, A. L. *J. Am. Chem. Soc.* **2000**, *122*, 2261. (n) Gilbertson, R. D.; Weakley, T. J. R.; Haley, M. M. *Chem.–Eur. J.* **2000**, *6*, 437.

(3) Examples of recent theoretical work: (a) Karton, A.; Iron, M. A.; van der Boom, M. E.; Martin, J. M. L. *J. Phys. Chem. A* **2005**, *109*, 5454. (b) Iron, M. A.; Lucassen, A. C. B.; Cohen, H.; van der Boom, M. E.; Martin, J. M. L. *J. Am. Chem. Soc.* **2004**, *126*, 11699. (c) Iron, M. A.; Martin, J. M. L.; van der Boom, M. E. *Chem. Commun.* **2003**, 132. (d) Iron, M. A.; Martin, J. M. L.; van der Boom, M. E. *J. Am. Chem. Soc.* **2003**, *125*, 13020. (e) Iron, M. A.; Martin, J. M. L.; van der Boom, M. E. *J. Am. Chem. Soc.* **2003**, *125*, 11702. (f) Huang, Y. Z.; Yang, S. Y.; Li, X. Y. *Chin. J. Chem. Phys.* **2003**, *16*, 440.

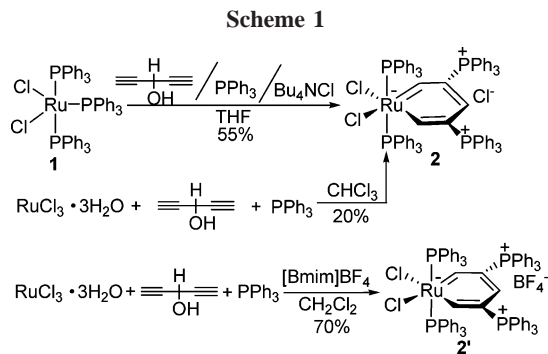
(4) Elliott, G. P.; Roper, W. R.; Waters, J. M. *J. Chem. Soc., Chem. Commun.* **1982**, 811.

(5) Rickard, C. E. F.; Roper, W. R.; Woodgate, S. D.; Wright, L. J. *Angew. Chem., Int. Ed.* **2000**, *39*, 750.

(6) Rickard, C. E. F.; Roper, W. R.; Woodgate, S. D.; Wright, L. J. *J. Organomet. Chem.* **2001**, *623*, 109.

(7) Xia, H.; He, G.; Zhang, H.; Wen, T. B.; Sung, H. H. Y.; Williams, I. D.; Jia, G. *J. Am. Chem. Soc.* **2004**, *126*, 6862.

(8) Additional examples: (a) Wu, H. P.; Lanza, S.; Weakley, T. J. R.; Haley, M. M. *Organometallics* **2002**, *21*, 2824. (b) Gilbertson, R. D.; Weakley, T. J. R.; Haley, M. M. *J. Am. Chem. Soc.* **1999**, *121*, 2597. (c) Bleeke, J. R.; Xie, Y. F.; Peng, W. J.; Chiang, M. *J. Am. Chem. Soc.* **1989**, *111*, 4118. (d) Bleeke, J. R.; Behm, R. *J. Am. Chem. Soc.* **1997**, *119*, 8503. (e) Bleeke, J. R.; Behm, R.; Xie, Y. F.; Chiang, M. Y.; Robinson, K. D.; Beatty, A. M. *Organometallics* **1997**, *16*, 606, and references therein.



and chromobenzene^{16b} have been proposed as reactive intermediates, but no direct observations of such species have been made.

In this work, we have been able to isolate a thermally stable ruthenabenzene from the one-pot reaction of inorganic salt RuCl_3 with $\text{HC}\equiv\text{CCH}(\text{OH})\text{C}\equiv\text{CH}$ and PPh_3 in high yield. Through ligand substitution reactions, we have prepared a series of stable ruthenabenzenes, including the first non-metal-coordinated bisruthenabenzene. We have also studied the electrochemical properties of ruthenabenzene and bisruthenabenzene by cyclic

(9) Other complexes closely related to metallabenzenes. Isometallabenzenes: (a) Barrio, P.; Esteruelas, M. A.; Onate, E. *J. Am. Chem. Soc.* **2004**, *126*, 1946. Metallabenzavalenes: (b) Wu, H. P.; Weakley, T. J. R.; Haley, M. M. *Organometallics* **2002**, *21*, 4320. Metallathiabenzenes: (c) Bleeke, J. R.; Hinkle, P. V.; Shokeen, M.; Rath, N. P. *Organometallics* **2004**, *23*, 4139. (d) Bleeke, J. R.; Hinkle, P. V.; Rath, N. P. *Organometallics* **2001**, *20*, 1939. (e) Bleeke, J. R.; Hinkle, P. V.; Rath, N. P. *J. Am. Chem. Soc.* **1999**, *121*, 595. (f) Bianchini, C.; Meli, A.; Peruzzini, M.; Vizza, F.; Moneti, S.; Herrera, V.; Sanchez-Delgado, R. A. *J. Am. Chem. Soc.* **1994**, *116*, 4370. (g) Bianchini, C.; Meli, A.; Peruzzini, M.; Vizza, F.; Frediani, P.; Herrera, V.; Sanchez-Delgado, R. A. *J. Am. Chem. Soc.* **1993**, *115*, 2731. (h) Jones, W. D.; Chin, R. M. *J. Am. Chem. Soc.* **1992**, *114*, 9851. (i) Chin, R. M.; Jones, W. D. *Angew. Chem., Int. Ed. Engl.* **1992**, *31*, 357. (j) Chen, J.; Daniels, L. M.; Angelici, R. J. *J. Am. Chem. Soc.* **1990**, *112*, 199. Metallapyridines: (k) Weller, K. J.; Filippov, I.; Briggs, P. M.; Wigley, D. E. *Organometallics* **1998**, *17*, 322. Metallapyryliums: (l) Bleeke, J. R.; Blanchard, J. M. B.; Donnay, E. *Organometallics* **2001**, *20*, 324. (m) Bleeke, J. R.; Blanchard, J. M. B. *J. Am. Chem. Soc.* **1997**, *119*, 5443. Metallabenzynes: (n) Wen, T. B.; Hung, W. Y.; Sung, H. H. Y.; Williams, I. D.; Jia, G. *J. Am. Chem. Soc.* **2005**, *127*, 2856. (o) Wen, T. B.; Ng, S. M.; Hung, W. Y.; Zhou, Z. Y.; Lo, M. F.; Shek, L. Y.; Williams, I. D.; Lin, Z.; Jia, G. *J. Am. Chem. Soc.* **2003**, *125*, 884. (p) Wen, T. B.; Zhou, Z. Y.; Jia, G. *Angew. Chem., Int. Ed.* **2001**, *40*, 1951. (q) Roper, W. R. *Angew. Chem., Int. Ed.* **2001**, *40*, 2440.

(10) Thorn, D. L.; Hoffman, R. *Nouv. J. Chim.* **1979**, *3*, 39.

(11) Coordinated metallabenzenes with a metal of the first transition series: (a) Hein, J.; Jeffery, J. C.; Scherwood, P.; Stone, F. G. A. *J. Chem. Soc., Dalton Trans.* **1987**, 2211. (b) Bertling, U.; Englert, U.; Salzer, A. *Angew. Chem., Int. Ed. Engl.* **1994**, *33*, 1003.

(12) Coordinated ruthenabenzenes: (a) Bosch, H. W.; Hund, H.-U.; Nietlispach, D.; Salzer, A. *Organometallics* **1992**, *11*, 2087. (b) Lin, W.; Wilson, S. R.; Girolami, G. S. *J. Am. Chem. Soc., Chem. Commun.* **1993**, 284. (c) Lin, W.; Wilson, S. R.; Girolami, G. S. *Organometallics* **1997**, *16*, 2356. (d) Englert, U.; Podewils, F.; Schiffers, I.; Salzer, A. *Angew. Chem., Int. Ed.* **1998**, *37*, 2134. (e) Liu, S. H.; Ng, W. S.; Chu, H. S.; Wen, T. B.; Xia, H. P.; Zhou, Z. Y.; Lau, C. P.; Jia, G. *Angew. Chem., Int. Ed.* **2002**, *41*, 1589. (f) Bruce, M. I.; Zaitseva, N. N.; Skelton, B. W.; White, A. H. *J. Chem. Soc., Dalton Trans.* **2002**, 1678. (g) Effertz, U.; Englert, U.; Podewils, F.; Salzer, A.; Wagner, T.; Kaupp, M. *Organometallics* **2003**, *22*, 264.

(13) Other coordinated metallabenzenes with a metal of the second transition series: (a) Kralick, M. S.; Rheingold, A. L.; Ernst, R. D. *Organometallics* **1987**, *6*, 2612. (b) Kralick, M. S.; Rheingold, A. L.; Hutchinson, J. P.; Freeman, J. W.; Ernst, R. D. *Organometallics* **1996**, *15*, 551.

(14) (a) Profflet, R. D.; Fanwick, P. E.; Rothwell, I. P. *Angew. Chem., Int. Ed. Engl.* **1992**, *31*, 1261. (b) Riley, P. N.; Profflet, R. D.; Salberg, M. M.; Fanwick, P. E.; Rothwell, I. P. *Polyhedron* **1998**, *17*, 773.

(15) (a) Yand, J.; Jones, W. M.; Dixon, J. K.; Allison, N. T. *J. Am. Chem. Soc.* **1995**, *117*, 9776. (b) Yang, J.; Yin, J.; Abboud, K. A.; Jones, W. M. *Organometallics* **1994**, *13*, 971.

(16) (a) Ferede, R.; Allison, N. T. *Organometallics* **1983**, *2*, 463. (b) Sivavec, T. M.; Katz, T. J. *Tetrahedron Lett.* **1985**, *26*, 2159.

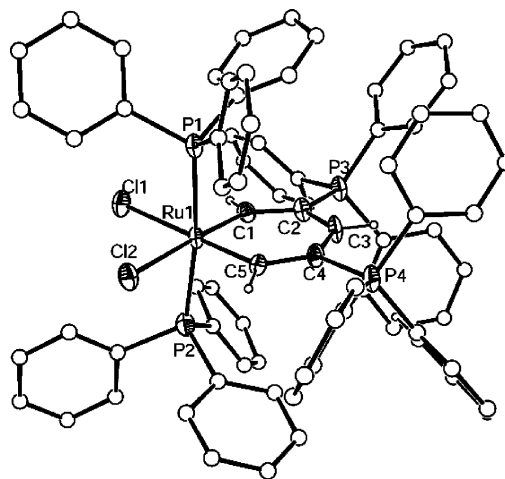


Figure 1. X-ray structure of complex **2**. Counteranion and some of the hydrogen atoms are omitted for clarity. Selected bond distances (Å) and angles (deg): Ru1–C1 1.922(5), C1–C2 1.382(7), C2–C3 1.395(7), C3–C4 1.378(7), C4–C5 1.391(7), C5–Ru1 1.911(5), C2–P3 1.790(5), C4–P4 1.792(5), Ru1–P1 2.4148(15), Ru1–P2 2.3926(15), Ru1–Cl1 2.5046(13), Ru1–Cl2 2.5196(13); C1–Ru1–P1 92.25(15), C1–Ru1–P2 93.10(15), C5–Ru1–P1 93.17(15), C5–Ru1–P2 91.63(15), P1–Ru1–P2 172.78(5), Cl1–Ru1–Cl2 94.85(5), C1–C2–P3 123.3(4), C3–C4–P4 114.6(4), C3–C2–P3 114.3(4), C5–C4–P4 122.2(4), C1–Ru1–C5 90.4(2), C2–C1–Ru1 129.5(4), C1–C2–C3 122.2(5), C2–C3–C4 125.2(5), C3–C4–C5 123.2(4), C4–C5–Ru1 128.6(4).

voltammetry. A preliminary communication of this work has been published.¹⁷

Results and Discussion

One-Pot Reaction of Ruthenium Compounds with $\text{HC}\equiv\text{CCH}(\text{OH})\text{C}\equiv\text{CH}$. Treatment of $\text{RuCl}_2(\text{PPh}_3)_3$ ¹⁸ with $\text{HC}\equiv\text{CCH}(\text{OH})\text{C}\equiv\text{CH}$ and PPh_3 leads to the formation of the stable greenish ruthenabenzene **2**, which can be isolated in 55% yield (Scheme 1).

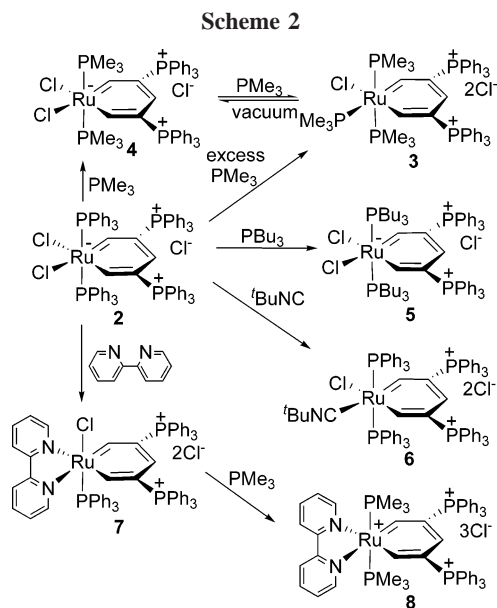
The structure of **2** has been confirmed by X-ray diffraction (Figure 1). The solution NMR spectroscopic data and elemental analysis are consistent with the solid-state structure. In particular, the ³¹P{¹H} NMR spectrum in CDCl_3 showed two singlets at 18.2 and 8.1 ppm assignable to CPh_3 and RuPh_3 , respectively. The presence of the metallacycle is clearly indicated by the ¹H and ¹³C NMR data. The ¹H NMR spectrum in CDCl_3 showed the characteristic RuCH signal at 17.5 ppm and the γ -CH signal at 8.2 ppm. The ¹H NMR chemical shift of the RuCH signal (17.5 ppm) is significantly downfield compared to that of the vinyl complex $\text{Ru}[\text{CH}=\text{CH}(\text{C}_6\text{H}_4\text{-}p\text{-OMe})]\text{Cl}(\text{CO})(\text{PPh}_3)_2$ (8.13

(17) Zhang, H.; Xia, H.; He, G.; Wen, T. B.; Gong, L.; Jia, G. *Angew. Chem., Int. Ed.* **2006**, *45*, 2920.

(18) Hallman, P. S.; Stephenson, T. A.; Wilkinson, G. *Inorg. Synth.* **1970**, *12*, 237.

(19) Maruyama, Y.; Yamamura, K.; Sagawa, T.; Katayama, H.; Ozawa, F. *Organometallics* **2000**, *19*, 1308.

(20) (a) Sanford, M. S.; Henling, L. M.; Day, M. W.; Grubbs, R. H. *Angew. Chem., Int. Ed.* **2000**, *39*, 3451. (b) Kingsbury, J. S.; Harrity, J. P. A.; Bonitatebus, P. J., Jr.; Hoveyda, A. H. *J. Am. Chem. Soc.* **1999**, *121*, 791. (c) Garber, S. B.; Kingsbury, J. S.; Gray, B. L.; Hoveyda, A. H. *J. Am. Chem. Soc.* **2000**, *122*, 8168. (d) Kingsbury, J. S.; Garber, S. B.; Giftos, J. M.; Gray, B. L.; Okamoto, M. M.; Farrer, R. A.; Fourkas, J. T.; Hoveyda, A. H. *Angew. Chem., Int. Ed.* **2001**, *40*, 4251. (e) Van Veldhuizen, J. J.; Garber, S. B.; Kingsbury, J. S.; Hoveyda, A. H. *J. Am. Chem. Soc.* **2002**, *124*, 4954. (f) Van Veldhuizen, J. J.; Gillingham, D. G.; Garber, S. B.; Kataoka, O.; Hoveyda, A. H. *J. Am. Chem. Soc.* **2003**, *125*, 12502. (g) Gillingham, D. G.; Kataoka, O.; Garber, S. B.; Hoveyda, A. H. *J. Am. Chem. Soc.* **2004**, *126*, 12288.



ppm),¹⁹ but is close to those of ruthenium carbene complexes, for example, $(\text{PCy}_3)(\text{RO})_2\text{Ru}=\text{CHPh}$ ($\text{R} = \text{tBu}$, 15.5 ppm; $\text{R} = \text{C}(\text{CF}_3)_2(\text{CH}_3)$, 17.5 ppm; $\text{R} = \text{C}(\text{CF}_3)_3$, 19.2 ppm),^{20a} $\text{Cl}_2\text{Ru}(\text{=CH-}o\text{-OMeC}_6\text{H}_4)(\text{PPh}_3)_2$ (16.16 ppm),^{20b} $\text{Cl}_2\text{Ru}(\text{=CH-}o\text{-OMeC}_6\text{H}_4)\text{PR}_3$ ($\text{R} = \text{Ph}$, 16.82 ppm; $\text{R} = \text{Cy}$, 17.36 ppm),^{20b} $\text{Cl}_2\text{Ru}(\text{=CH-}o\text{-O-}i\text{-PrC}_6\text{H}_4)(\text{PPh}_3)_2$ ($\text{R} = \text{Ph}$, 16.76 ppm; $\text{R} = \text{Cy}$, 17.44 ppm),^{20b} $\text{Cl}_2\text{Ru}(\text{=CH-}o\text{-OMeC}_{10}\text{H}_6)\text{PCy}_3$ (17.52 ppm),^{20b} and $(4,5\text{-dihydroIMES})\text{Cl}_2\text{Ru}=\text{CH-}o\text{-O-}i\text{-PrC}_6\text{H}_4$ (16.56 ppm),^{20c} indicating that the RuCH in **2** has carbene character. In the $^{13}\text{C}\{^1\text{H}\}$ NMR spectrum (in CD_2Cl_2), the signals of RuCH , CPh_3 , and $\gamma\text{-CH}$ are observed at 284.3, 108.3, and 146.0 ppm, respectively. The NMR data suggest that the six-membered metallacycle of **2** has a delocalized symmetrical structure.

Ruthenabenzene **2** represents a rare example of thermally stable metallabenzene with a transition metal of the second transition series. As will be discussed below, only when heated to 120 °C could the decomposition of **2** be observed. The higher thermal and air stability of ruthenabenzene **2** are probably related to the protecting effect of the bulky phosphine substituents and/or ligands. The electronics may also play an important role in the stability of **2**.

We have found that **2** can even be obtained from the one-pot reaction of RuCl_3 , PPh_3 , and $\text{HC}\equiv\text{CCH}(\text{OH})\text{C}\equiv\text{CH}$ in CHCl_3 , although the yield is low (ca. 20%).¹⁷ When the one-pot reaction of RuCl_3 , PPh_3 , and $\text{HC}\equiv\text{CCH}(\text{OH})\text{C}\equiv\text{CH}$ was carried out in the mixed solution of $[\text{Bmim}]\text{BF}_4$ (1-butyl-3-methylimidazolium tetrafluoroborate)/ CH_2Cl_2 (1:10, v/v), the yield of ruthenabenzene **2'** can be increased to 70% (Scheme 1). We also tried the reaction in the presence of other ionic liquids, such as $[\text{Bmim}]\text{PF}_6$ (1-butyl-3-methylimidazolium hexafluorophosphate), $[\text{Emim}]\text{BF}_4$ (1-ethyl-3-methylimidazolium tetrafluoroborate), and $[\text{Bmim}]\text{Cl}$ (1-butyl-3-methylimidazolium chloride). As showed by *in situ* NMR, the reactions in the presence of $[\text{Bmim}]\text{BF}_4$ and $[\text{Bmim}]\text{PF}_6$ are not air-sensitive and have no other side products. When the reaction is performed in the presence of $[\text{Emim}]\text{BF}_4$ and $[\text{Bmim}]\text{Cl}$, the formation of ruthenabenzene **2** also occurred, but the reactions are much slower and also produced other uncharacterized products. The formation of ruthenabenzene **2** starting from RuCl_3 in high yield represents a rare example of constructing metallabenzene from inorganic salts.

Ligand Substitution Reactions of Ruthenabenzene 2. An additional new, stable ruthenabenzene can be obtained by substitution reactions of complex **2**. Treatment of **2** with PMe_3

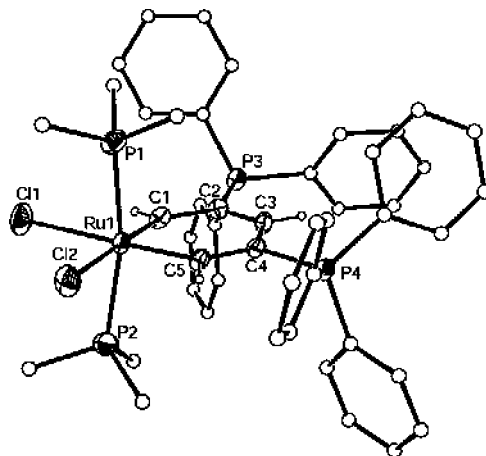


Figure 2. X-ray structure of complex **4**. Counteranion and some of the hydrogen atoms are omitted for clarity. Selected bond distances (Å) and angles (deg): $\text{Ru1}-\text{C1}$ 1.913(4), $\text{Ru1}-\text{C5}$ 1.908(4), $\text{Ru1}-\text{P1}$ 2.3768(15), $\text{Ru1}-\text{P2}$ 2.3604(15), $\text{Ru1}-\text{Cl1}$ 2.5519(14), $\text{Ru1}-\text{Cl2}$ 2.5205(13), $\text{P3}-\text{C2}$ 1.802(4), $\text{P4}-\text{C4}$ 1.789(4), $\text{C1}-\text{C2}$ 1.399(6), $\text{C2}-\text{C3}$ 1.388(6), $\text{C3}-\text{C4}$ 1.397(6), $\text{C4}-\text{C5}$ 1.381(6); $\text{C1}-\text{Ru1}-\text{P1}$ 93.55(14), $\text{C5}-\text{Ru1}-\text{P1}$ 94.26(14), $\text{C1}-\text{Ru1}-\text{P2}$ 98.22(14), $\text{C5}-\text{Ru1}-\text{P2}$ 93.08(14), $\text{P1}-\text{Ru1}-\text{P2}$ 166.11(5), $\text{Cl1}-\text{Ru1}-\text{Cl2}$ 91.49(5), $\text{C3}-\text{C2}-\text{P3}$ 117.9(3), $\text{C1}-\text{C2}-\text{P3}$ 119.2(3), $\text{C5}-\text{C4}-\text{P4}$ 119.8(3), $\text{C3}-\text{C4}-\text{P4}$ 116.3(3), $\text{C1}-\text{Ru1}-\text{C5}$ 90.09(19), $\text{Ru1}-\text{C1}-\text{C2}$ 129.5(3), $\text{C1}-\text{C2}-\text{C3}$ 122.9(4), $\text{C2}-\text{C3}-\text{C4}$ 123.6(4), $\text{C3}-\text{C4}-\text{C5}$ 123.9(4), $\text{C4}-\text{C5}-\text{Ru1}$ 129.5(3).

(2 equiv) produced complex **4** (Scheme 2). As suggested by *in situ* NMR, the reaction of **2** with excess PMe_3 (25 equiv) also produced complex **3**, an analogue of the reported osmabenzene $[\text{Os}(\text{CHC}(\text{PPh}_3)\text{CHC}(\text{PPh}_3)\text{CH})\text{Cl}(\text{PMe}_3)_3]\text{Cl}_2$.⁷ The $^{31}\text{P}\{^1\text{H}\}$ NMR spectrum of **3** in CDCl_3 showed four signals at 20.6, 17.1, -11.7, and -22.1 ppm assignable to CPh_3 and RuPMe_3 , respectively. The ^1H NMR spectrum of **3** in CDCl_3 showed the characteristic RuCH signal at 15.9 and 14.8 ppm. However, unlike the osmabenzene $[\text{Os}(\text{CHC}(\text{PPh}_3)\text{CHC}(\text{PPh}_3)\text{CH})\text{Cl}(\text{PMe}_3)_3]\text{Cl}_2$, one of the PMe_3 ligand in **3** is not tightly bound to ruthenium and could be easily removed under vacuum to give complex **4**. Thus pure samples of **3** could not be obtained.

The structure of **4** has also been confirmed by X-ray diffraction, and its molecular structure is depicted in Figure 2. In agreement with the solid-state structure, the $^{31}\text{P}\{^1\text{H}\}$ NMR spectrum showed one CPh_3 signal at 18.1 ppm and one RuPMe_3 signal at -13.9 ppm. The observation of two ^1H signals of the ring protons in the ^1H NMR spectrum (17.0 (RuCH) and 7.9 ($\gamma\text{-CH}$) ppm) and three ^{13}C signals of the metallacycle in the $^{13}\text{C}\{^1\text{H}\}$ NMR spectrum (279.6 (RuCH), 143.3 (CH), and 107.3 (CPh_3) ppm) verifies the symmetric structure of **4**.

Treatment of a solution of ruthenabenzene **2** in dichloromethane with PBU_3 produced ruthenabenzene **5** (Scheme 2). The structure of complex **5** can be inferred from its NMR spectroscopy. The $^{31}\text{P}\{^1\text{H}\}$ NMR spectrum in CDCl_3 showed the CPh_3 signal at 19.1 ppm and the RuPBU_3 signal at 5.8 ppm. Consistent with the proposed structure, the ^1H and ^{13}C NMR data associated with the metallacycle are similar to those of complex **4**.

Other thermally stable ruthenabenzene can also be obtained by substitution reactions of **2**. Addition of $t\text{BuNC}$ to a dichloromethane solution of **2** leads to the formation of the isocyanide-containing complex **6** (Scheme 2). The structure of ruthenabenzene **6** can be readily assigned on the basis of the NMR data. In particular, the $^{31}\text{P}\{^1\text{H}\}$ NMR spectrum showed three singlet peaks at 25.1 (RuPPh_3), 23.3 (CPh_3), and 18.3 (CPh_3) ppm. In the ^1H NMR spectrum, the two signals of RuCH appeared

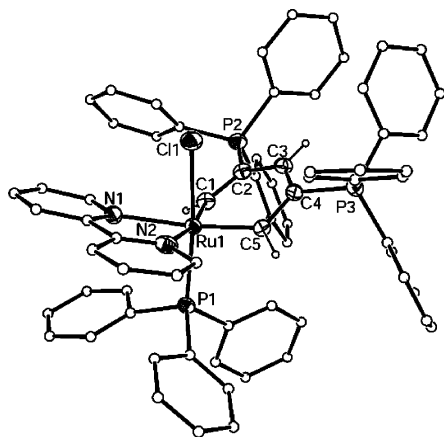


Figure 3. X-ray structure of complex **7**. Counteranion and some of the hydrogen atoms are omitted for clarity. Selected bond distances (Å) and angles (deg): Ru1–C1 1.935(4), C1–C2 1.382(6), C2–C3 1.387(7), C3–C4 1.396(7), C4–C5 1.407(6), C5–Ru1 1.914(4), C2–P2 1.793(5), C4–P3 1.790(5), Ru1–P1 2.3178(12), Ru1–Cl1 2.4407(13), Ru1–N1 2.210(4), Ru1–N2 2.189(4); C1–Ru1–P1 94.23(14), C1–Ru1–Cl1 89.00(14), C5–Ru1–P1 96.47(14), C5–Ru1–Cl1 88.76(14), P1–Ru1–Cl1 173.87(4), N1–Ru1–N2 74.51(16), C1–C2–P2 117.2(4), C3–C4–P3 118.3(3), C3–C2–P2 118.8(4), C5–C4–P3 118.4(3), C1–Ru1–C5 89.43(19), C2–C1–Ru1 123.9(3), C1–C2–C3 123.9(4), C2–C3–C4 123.6(4), C3–C4–C5 122.8(4), C4–C5–Ru1 123.5(3).

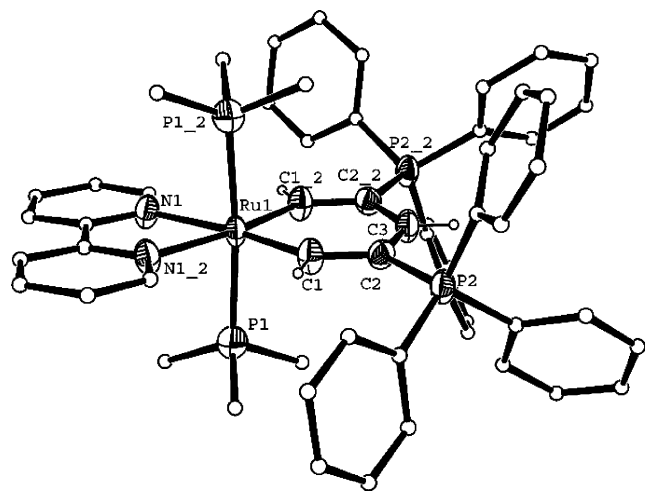
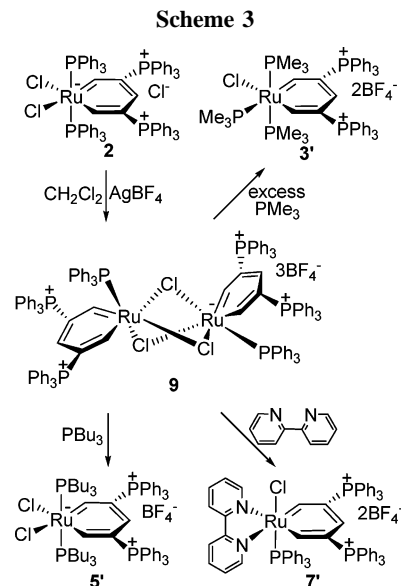


Figure 4. X-ray structure of complex **8**. Counteranion and some of the hydrogen atoms are omitted for clarity. Selected bond distances (Å) and angles (deg): Ru1–C1 1.916(4), Ru1–N1 2.187(3), Ru1–P1 2.3583(14), P2–C2 1.790(4), C1–C2 1.386(5), C2–C3 1.381(5), C1–Ru1–Cl1_2 88.2(2), C1–Ru1–P1 94.94(13), P1–Ru1–P1_2 174.95(6), C2–C1–Ru1 130.9(3), C1–C2–C3 123.0(4), C2–C3–C2_2 123.4(5). (Symmetry transformations used to generate equivalent atoms: 2 = $-x+3/4, -y+3/4, z$.)

at 15.6 and 15.5 ppm. In the $^{13}\text{C}\{^1\text{H}\}$ NMR spectrum, the five carbon signals of the metallacycle appeared at 286.1 (RuCH), 280.6 (RuCH), 149.1 (γ -CH), 113.7 (CPPH₃), and 113.6 (CPPH₃) ppm.

As judged on the basis of NMR data, treatment of **2** with 2,2'-dipyridyl led to the replacement of one chloride and one PPh₃ ligand to give ruthenabenzene **7** (Scheme 2). The structure of **7** has also been determined by X-ray diffraction (Figure 3). It is interesting that the metallabenzene ring of **7** is distorted with the ruthenium center tilted out of the plane of the C₅ backbone. The ruthenium center lies -0.6722 (56) Å out of



the plane of the ring carbon atoms (C1, C2, C3, C4, C5). The dihedral angle between this plane and the C1/Ru/C5 plane is 29.3° .

The tilt angle of metallacycle of **7** is even larger than that in the coordinated ruthenabenzene $[(\text{C}_5\text{H}_5)\text{Ru}(\mu\text{-C}_7\text{H}_9)\text{Ru}(\text{C}_5\text{Me}_5)(\text{CH}_3\text{CN})]\text{PF}_6$ (27.2°).^{12a} Although not common, other nonplanar metallabenzene are known. For example, in iridabenzene supported by the Tp ligand, the iridium metal is also bent by 0.57 to 0.76 Å out of the plane of the metallacyclic carbon atoms.^{2c,j} Recently, Lin and Jia also reported the similar distorted osmabenzene $[\text{Os}(\text{C}(\text{OR})\text{CH}=\text{C}(\text{Me})\text{C}(\text{SiMe}_3)=\text{CH})(\text{bipy})(\text{PPh}_3)_2]\text{OTf}$ (R = H, Me),^{2a} and their theoretical study suggests that the nonplanarity in their osmabenzene $[\text{Os}(\text{C}(\text{OR})\text{CH}=\text{C}(\text{Me})\text{C}(\text{SiMe}_3)=\text{CH})(\text{bipy})(\text{PPh}_3)_2]\text{OTf}$ is mainly due to electronic reasons. We presumed that the unsymmetric coordination environment of the ruthenium center (the difference of the bulky PPh₃ ligand and the small Cl ligand above and below the metallacycle) causes the nonplanarity in our ruthenabenzene **7**. The C–C bond distances of the C1–C5 chain are in the range 1.382(6)–1.407(6) Å, and the lack of significant alternations in the C–C bond distances suggests that **7** has a delocalized structure, although the metallacycle is not planar.

Treatment of **7** with PMe₃ in CH₂Cl₂ produced the ruthenabenzene **8** (Scheme 2). The structure of **8** has been confirmed by X-ray diffraction. The X-ray structure (Figure 4) clearly shows that the complex indeed has an essentially planar six-membered metallacycle with two PPh₃ substituents. The coplanarity is reflected by the small rms deviation (0.0261 Å) from the least-squares plane through the six atoms Ru1, C1, C2, C3, C1_2, and C2_2. The solution NMR spectroscopic data are consistent with the solid-state structure. In particular, the ¹H NMR spectrum showed a characteristic RuCH proton signal at 16.1 ppm, and the ¹³C{¹H} NMR spectrum showed the three carbon signals of the metallacycle at 291.0 (RuCH), 149.6 (γ -CH), and 114.5 (CPPH₃) ppm.

Preparation of a Bisruthenabenzene from Ruthenabenzene 2. Treatment of **2** with AgBF₄ in CH₂Cl₂ produced the bisruthenabenzene **9** (Scheme 3). As suggested by *in situ* NMR, treatment of **2** with excess HBF₄ (10 equiv) can also produce the bisruthenabenzene **9**. The ³¹P{¹H} NMR spectrum in CD₂-Cl₂ showed two CPPH₃ signals at 20.1 and 18.8 ppm and one RuPPh₃ signal at 34.6 ppm. The two characteristic RuCH signals at 16.1 and 16.0 ppm in the ¹H NMR spectrum of **9** are typical for our ruthenabenzene; for example, the RuCH signal of **2**

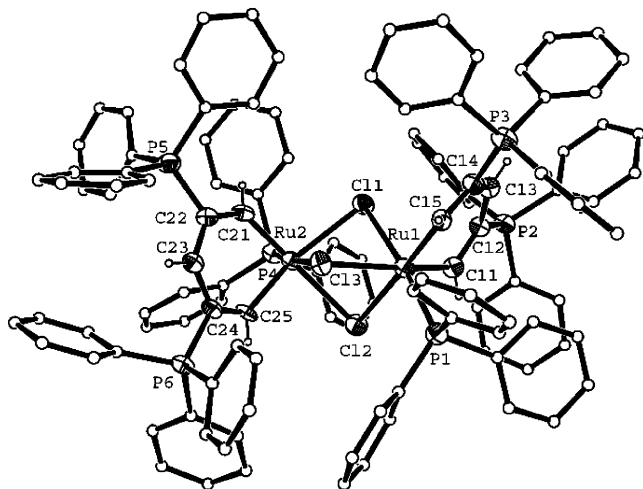
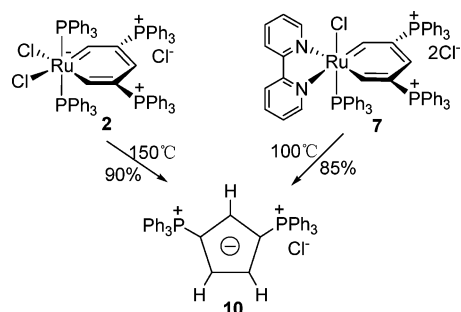


Figure 5. X-ray structure of complex **9**. Counteranion and some of the hydrogen atoms are omitted for clarity. Selected bond distances (Å) and angles (deg): Ru1–C11 1.912(4), Ru1–C15 1.909(4), Ru1–P1 2.3219(12), Ru1–Cl1 2.4594(11), Ru1–Cl2 2.5457(13), Ru1–Cl3 2.5216(12), Ru2–C21 1.888(4), Ru2–C25 1.927(4), Ru2–P4 2.3193(12), Ru2–Cl1 2.5263(12), Ru2–Cl2 2.5508(12), Ru2–Cl3 2.4786(11), P2–C12 1.782(4), P3–C14 1.787(5), P5–C22 1.778(4), P6–C24 1.798(4), C11–C12 1.391(6), C12–C13 1.386(6), C13–C14 1.393(6), C14–C15 1.406(7), C21–C22 1.408(6), C22–C23 1.384(6), C23–C24 1.407(6), C24–C25 1.367(6), C11–Ru1–C15 91.01(19), C12–C11–Ru1 123.7(3), C11–C12–C13 123.4(4), C12–C13–C14 124.0(4), C13–C14–C15 123.6(4), C14–C15–Ru1 124.2(3), Ru1–C11–Ru2 83.00(4), Ru1–Cl2–Ru2 80.82(4), Ru1–Cl3–Ru2 82.71(4), C21–Ru2–C25 90.81(19), C22–C21–Ru2 123.4(3), C21–C22–C23 122.9(4), C22–C23–C24 123.5(4), C23–C24–C25 124.3(4), C24–C25–Ru2 122.2(3).

appears at 17.5 ppm. The $^{13}\text{C}\{^1\text{H}\}$ NMR spectrum showed five signals at 292.3, 289.1 (RuCH), 145.5 (γ -CH), and 117.3, 115.9 (CPPh₃) ppm for the carbons of the two metallacyclic rings. On the basis of the solution NMR spectroscopic data, the structure could not be defined. Thus an X-ray diffraction study was carried out.

As shown in Figure 5, the X-ray diffraction study confirms that complex **9** contains two six-membered metallacycles connected by three chloro bridges. The Ru–Cl bond distances of the chloro bridges of **9** are in the range 2.4594(11)–2.5508(12) Å, which is similar to the reported bimetallic ruthenium complexes with three chloro bridges.²¹ The metallacycles of complex **9** deviate significantly from planarity, as reflected by the sum of angles in the six-membered rings (709.9° and 707.1°), which are significantly smaller than the ideal value of 720°. The mean deviation from the least-squares plane through the C11–C15 chain is 0.0232 (the relevant value in C21–C25 chain is 0.0098). Ru1 is out of the plane of the metallacyclic carbon atoms by –0.5974 Å (the relevant value of Ru2 is 0.6735 Å). The dihedral angle between the C11–C15 plane and the C11/Ru1/C15 plane is 26.4°, which is a little smaller than that in complex **7**, and the relevant dihedral angle of the Ru2 metal-

Scheme 4



lacycle is 30.1°, which is even larger than that in complex **7**. However, the two metallacycles of **9** still have a delocalized structure, as reflected by the C–C bond distances of the C11–C15 chain, which are in the range 1.386(6)–1.406(7) Å (C21–C15 chain: 1.367(6)–1.408(6) Å), and there is no C–C bond distance alternation. Although the nonplanarity of coordinated metallabenzene is usual,^{11–13} most of the free metallabenzene are coplanar. The unsymmetric coordination environment of the ruthenium centers of **9** is similar to the ruthenium center of **7**, which is regarded as the reason for the distorted metallacycle.

Several coordinated ruthenabenzene,¹² including Salzer's bimetallic sandwich complex,^{12d,g} have been previously isolated and well characterized. However, isolation of a non-metal-coordinated bimetallic ruthenabenzene has not been reported. To the best of our knowledge, this is the first structurally characterized non-metal-coordinated bimetallic ruthenabenzene.

Complex **9** is a green solid. It is air-stable and can be kept for several days without appreciable decomposition either in the solid state or in solution at room temperature. Since the stability of complex **9** is notable, we expected to prepare additional new, stable non-metal-coordinated bisruthenabenzene through substitution reactions of complex **9**. However, when **9** is subjected to substitution reactions, it cannot give new bisruthenabenzene, but the same monometallacycle products of substitution reactions of complex **2**.

Thermal Decomposition Reactions of Ruthenabenzene.

To test the thermal stability of ruthenabenzene **2**, we initially heated the solid sample of **2** at 100 °C in the air for 5 h. Its thermal stability is so remarkable that the sample remains nearly unchanged. When we raised the temperature to 120 °C, as suggested by *in situ* NMR, it produced a mixture of species with **10** as the dominant product. **10** could be isolated as a light yellow solid in 90% yield when a solid sample of complex **2** was heated at 150 °C for 5 h (Scheme 4). When a solid sample of complex **7** was heated at 100 °C for 2 h, it could also produce **10** in 85% yield (Scheme 4). We indeed found that complex **10** was the decomposition product of ruthenabenzene **2**, which could be observed as a minor product in the ligand substitution reactions of ruthenabenzene **2**.

The structure of **10** has been confirmed by an X-ray diffraction study. As shown in Figure 6, **10** contains a planar five-membered carbon cycle with two PPh₃ substituents. The coplanarity is reflected by the very small deviations (0.0022 Å) from the rms planes of the best fit through the five atoms C1, C2, C3, C4, and C5. In addition, the sum of the internal angles around the ring is 540°, which is equal to the value required for planar pentagon. The C–C bond distances around the ring are similar and are in the range 1.360(4)–1.407(4) Å. The lack of significant alternations in the C–C bond distances suggests that **10** has a delocalized structure. In agreement with the solid-state structure, the $^{31}\text{P}\{^1\text{H}\}$ NMR spectrum in CDCl₃ showed the CPPh₃ signal at 14.2 ppm. The ^1H NMR spectrum

(21) Examples of some bimetallic ruthenium complexes with three chloro bridges: (a) Quebatte, L.; Haas, M.; Solari, E.; Scopelliti, R.; Nguyen, Q. T.; Severin, K. *Angew. Chem., Int. Ed.* **2005**, *44*, 1084. (b) Gauthier, S.; Quebatte, L.; Scopelliti, R.; Severin, K. *Chem.–Eur. J.* **2004**, *10*, 2811. (c) Faure, M.; Maurette, L.; Donnadiou, B.; Lavigne, G. *Angew. Chem., Int. Ed.* **1999**, *38*, 4. (d) Fabre, S.; Kalck, P.; Lavigne, G. *Angew. Chem., Int. Ed. Engl.* **1997**, *36*, 1092. (e) Bino, A.; Gotton, F. A. *J. Am. Chem. Soc.* **1980**, *102*, 608. (f) Cotton, F. A.; Torralba, R. C. *Inorg. Chem.* **1991**, *30*, 2196. (g) Mashima, K.; Komura, N.; Yamagata, T.; Tani, K. *Inorg. Chem.* **1997**, *36*, 2908.

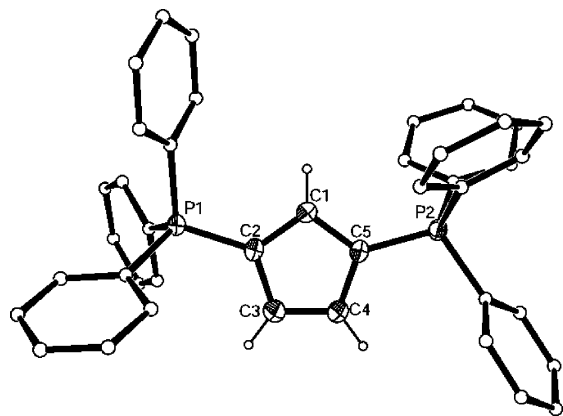


Figure 6. X-ray structure of complex **10**. Counteranion and some of the hydrogen atoms are omitted for clarity. Selected bond distances (Å) and angles (deg): P1–C2 1.738(3), P2–C5 1.732(2), C1–C2 1.385(4), C2–C3 1.407(4), C3–C4 1.360(4), C4–C5 1.406(4), C5–C1 1.400(3); C1–C2–P1 126.5(2), C3–C2–P1 125.1(2), C1–C5–P2 127.9(2), C4–C5–P2 124.06(19), C2–C1–C5 107.2(2), C1–C2–C3 108.3(2), C2–C3–C4 108.3(2), C3–C4–C5 108.2(2), C4–C5–C1 108.0(2).

in CDCl_3 showed two CH signals at 6.2 and 6.6 ppm. The ^{13}C - $\{^1\text{H}\}$ NMR spectrum showed three signals at 122.9 ($\text{CHCHC}(\text{PPh}_3)$), 121.1 ($\text{C}(\text{PPh}_3)\text{CHC}(\text{PPh}_3)$), and 92.8 ($\text{C}(\text{PPh}_3)$) ppm for the carbons of the ring.

As the thermal decomposition product of ruthenabenzene **2**, **10** has a more notable thermal stability such that the solid sample remains nearly unchanged after heating at 200 °C for 4 h in the air. A large number of substituted cyclopentadienyl ligands have been utilized to synthesize various metallocenes. Only a few stable Cp^- ions have been successfully isolated and well characterized, for example, $[(\text{C}_6\text{H}_5)_4\text{As}^+(\text{C}_5(\text{SCH}_3)_5)^-]$,^{22a} $[\text{C}_5(\text{CF}_3)_4(\text{OPR}_3)]$,^{22b} $[(\text{Me}_2\text{N})_3\text{S}^+\text{C}_5\text{H}_5^-]$,^{22c} $[\text{C}_5(\text{C}_6\text{H}_5)_4(\text{NC}_5\text{H}_5)]$,^{22d} and $\text{H}[4\text{-RC}_5\text{H}_2\text{-1,2-(C}(\text{Ph})\text{NH}_2)]$ ($\text{R} = \text{H}$ or SiMe_3).^{22e} Like the stable ruthenabenzene **2**, the protecting effect of the bulky phosphoniums may play an important role in the high thermal and air stability of **10**.

Electrochemical Study. While many theoretical studies and various synthetic methods of metallabenzenes have been reported, there are no reports on electrochemical studies of metallabenzenes. Our ruthenabenzene and bisruthenabenzene are composed of several redox-active units. To probe the redox behavior, cyclic voltammograms of ruthenabenzene **2** and bisruthenabenzene **9** were collected in dichloromethane containing 0.10 M Bu_4NClO_4 as the supporting electrolyte.

Scanning in the positive potential direction, **2** undergoes a redox process (A) with $E_{\text{p,a}} = 0.79$ V, $\Delta E_{\text{p}} = 112$ mV, when the scan rate is 100 mV/s (see the cyclic voltammogram shown in Figure 7). The ΔE_{p} values change from 70 to 130 mV, the $i_{\text{pa}}/i_{\text{pc}}$ ratio > 1 , and the ratio becomes larger as the scan rate varies from 20 to 150 mV/s (Figure 8). Complex **2** exhibits a linear dependence of the peak current on the square root of the scan rate ($\nu^{1/2}$) (Figure 8). These results indicate that the quasi-reversible oxidation process (A) is followed by a chemical reaction of the oxidized species. The oxidation wave may be assigned to the formation of $[\text{Ru}(\text{CHC}(\text{PPh}_3)\text{CHC}(\text{PPh}_3)\text{CH})-$

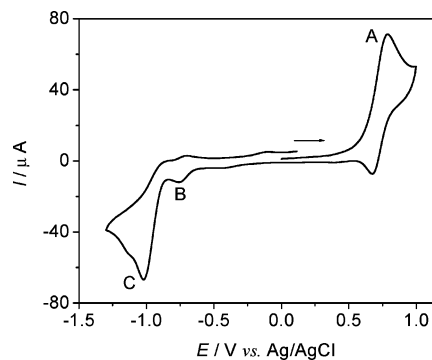


Figure 7. Cyclic voltammogram of 3 mM complex **2** measured in CH_2Cl_2 with 0.1 M Bu_4NClO_4 as supporting electrolyte at a scan rate of 100 mV/s.

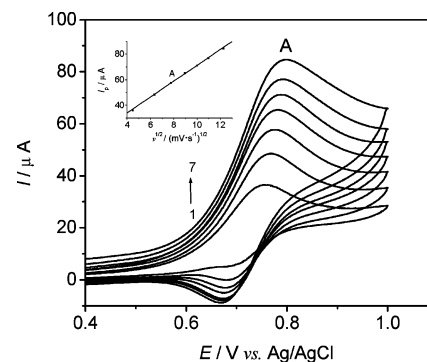


Figure 8. Voltammogram of complex **2** recorded in CH_2Cl_2 with 0.1 M Bu_4NClO_4 as supporting electrolyte, scan rate: (1) 20, (2) 40, (3) 60, (4) 80, (5) 100, (6) 120, (7) 150 mV/s. Inset: plot of wave A current vs the square root of scan rate.

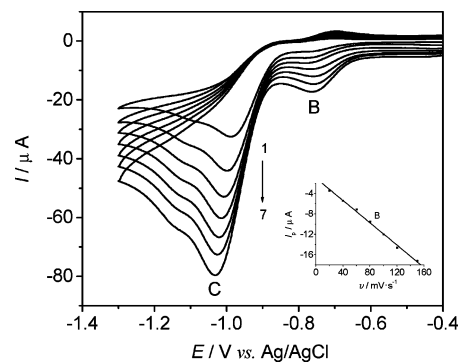


Figure 9. Voltammogram of complex **2** recorded in CH_2Cl_2 with 0.1 M Bu_4NClO_4 as supporting electrolyte, scan rate: (1) 20, (2) 40, (3) 60, (4) 80, (5) 100, (6) 120, (7) 150 mV/s. Inset: plot of wave B current vs scan rate.

$\text{Cl}_2(\text{PPh}_3)_2]^{2+}$. When voltammetric sweeping is carried out in the negative potential direction (Figure 7), two waves for complex **2** appear at -0.75 and -1.02 V, respectively. The peak current of the first wave (B) is found to be linear with scan rate (ν) in the range 20–150 mV/s (Figure 9), so we can presume that the first wave is considered as one prewave;²³ that is, the reduced product is strongly adsorbed on the glassy carbon electrode. The second reduction wave (C) is an irreversible process because there is no corresponding oxidation current on the return scan (Figure 9).

The electrochemical behavior of bisruthenabenzene **9** is quite different from that of ruthenabenzene **2**. The anodic CV scan of **9** (Figure 10) shows that the complex is not oxidized in the

(22) Examples of some stable Cp^- ions: (a) Wudl, F.; Nalewajek, D.; Rotella, F. J.; Gebert, E. *J. Am. Chem. Soc.* **1981**, *103*, 5885. (b) Burk, M. J.; Calabrese, J. C.; Davidson, F.; Harlow, R. L.; Roe, D. C. *J. Am. Chem. Soc.* **1991**, *113*, 2209. (c) Wessel, J.; Behrens, U.; Lork, E.; Mews, R. *Angew. Chem., Int. Ed. Engl.* **1995**, *34*, 443. (d) Bock, H.; Nick, S.; Nather, C.; Gobel, I.; John, A.; Kleine, M. *Liebigs Ann.* **1995**, 105. (e) Etkin, N.; Ong, D. M.; Stephan, D. W. *Organometallics* **1998**, *17*, 3656.

(23) Wopschall, R. H.; Shain, I. *Anal. Chem.* **1967**, *39*, 1514.

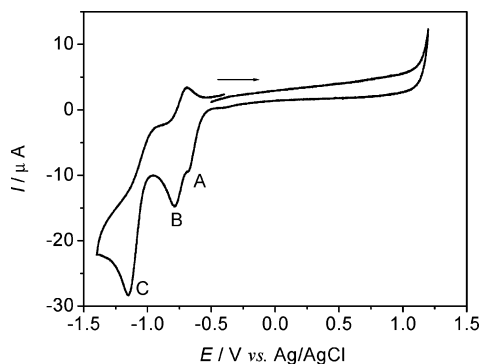


Figure 10. Cyclic voltammogram of 1 mM complex **9** measured in CH_2Cl_2 with 0.1 M Bu_4NClO_4 as supporting electrolyte at a scan rate of 100 mV/s.

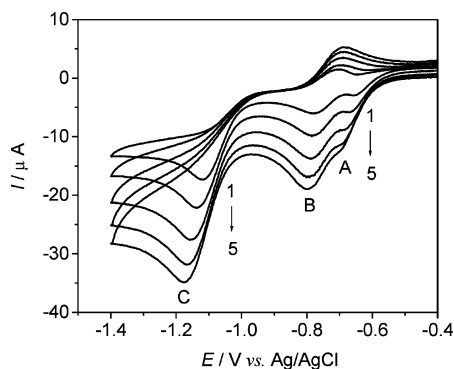


Figure 11. Voltammogram of complex **9** recorded in CH_2Cl_2 with 0.1 M Bu_4NClO_4 as supporting electrolyte, scan rate: (1) 20, (2) 50, (3) 100, (4) 150, (5) 200 mV/s.

range from -0.50 to $+1.00$ V, which indicates that bisruthenabenzene is more difficult to oxidize in contrast to ruthenabenzene. Two successive reduction peaks are observed at -0.68 (A) and -0.79 V (B) (Figure 10), which gradually overlap with increasing scan rate (Figure 11). These two successive processes (A, B) may be attributed to the reduction of $\{[\text{Ru}(\text{CHC}(\text{PPh}_3)\text{CHC}(\text{PPh}_3)\text{CH})(\text{PPh}_3)_2(\mu\text{-Cl})_3(\text{BF}_4)_3]^{3+}$ to $\{[\text{Ru}(\text{CHC}(\text{PPh}_3)\text{CHC}(\text{PPh}_3)\text{CH})(\text{PPh}_3)_2(\mu\text{-Cl})_3(\text{BF}_4)_3]^{2+}$ and $\{[\text{Ru}(\text{CHC}(\text{PPh}_3)\text{CHC}(\text{PPh}_3)\text{CH})(\text{PPh}_3)_2(\mu\text{-Cl})_3(\text{BF}_4)_3]^{1+}$, respectively. Observation of the two successive reduction waves (A, B) for complex **9** may imply that there is slightly electronic interaction between the two metal centers through the chloro bridges. A similar interaction of two ruthenium centers can be observed in the reported chloro-bridged dinuclear ruthenium complexes.^{21f,g} Following the two successive reduction waves (A, B), complex **9** exhibits one irreversible reduction process at -1.15 V (C) because there is no corresponding oxidation current on the return scan (Figure 11), similar to complex **2** at -1.02 V (C).

Conclusion

Most of the previously well-characterized stable metallabenzene are those with a transition metal of the third transition series. Well-characterized metallabenzene with a metal of the first and the second transition series are still very rare. In this work, the air-stable and thermo-stable ruthenabenzene $[\text{Ru}(\text{CHC}(\text{PPh}_3)\text{CHC}(\text{PPh}_3)\text{CH})\text{Cl}_2(\text{PPh}_3)_2\text{Cl}$ (**2**) can be obtained from the one-pot reaction of $\text{RuCl}_2(\text{PPh}_3)_3$ or inorganic salt RuCl_3 with $\text{HC}\equiv\text{CCH}(\text{OH})\text{C}\equiv\text{CH}$ and PPh_3 in high yield. Its thermal stability is so remarkable that the sample remains nearly unchanged when we heat the solid sample of **2** at 100 °C in the air for 5 h. Ligand substitution reactions of **2** produce a series

of new, stable ruthenabenzenes **4**, **5**, **6**, **7**, and **8**. Most of our ruthenabenzenes have a planar metallacycle, while the unsymmetric coordination environment of the ruthenium center causes the nonplanarity in ruthenabenzene **7**. Treatment of **2** with AgBF_4 produces the first stable non-metal-coordinated bismetallabenzene **9**. The electrochemical studies show that complex **2** is more easily oxidized than complex **9**, and the metal centers in the bisruthenabenzene **9** slightly interact with each other. During the investigation of the thermal stability of ruthenabenzene **2**, the thermal decomposition product **10** (Cp^- ion derivative) was isolated and well characterized. **10** has a more notable thermal stability such that the solid sample remains nearly undecomposed after heating at 200 °C for 4 h in the air.

Experimental Section

All manipulations were carried out at room temperature under a nitrogen atmosphere using standard Schlenk techniques, unless otherwise stated. Solvents were distilled under nitrogen from sodium benzophenone (hexane, ether, THF) or calcium hydride (CH_2Cl_2 , CHCl_3). The starting materials $\text{RuCl}_2(\text{PPh}_3)_3$ ¹⁸ and $\text{HC}\equiv\text{CCH}(\text{OH})\text{C}\equiv\text{CH}$ ²⁴ were synthesized by literature procedures. Column chromatography was performed on silica gel (300–400 mesh) or alumina gel (200–300 mesh). NMR experiments were performed on a Varian Unity Plus-500 spectrometer (^1H 500.40 MHz; ^{13}C 125.7 MHz; ^{31}P 202.4 MHz) or a Bruker ARX-300 spectrometer (^1H 300.13 MHz; ^{13}C 75.5 MHz; ^{31}P 121.5 MHz). ^1H and ^{13}C NMR chemical shifts are relative to TMS, and ^{31}P NMR chemical shifts are relative to 85% H_3PO_4 . Elemental analyses data were obtained on a Thermo Quest Italia S.P.A. EA 1110.

Cyclic voltammetry was performed at room temperature (25 °C) under N_2 atmosphere in freshly distilled CH_2Cl_2 containing 0.1 M Bu_4NClO_4 (TBAP), using a CHI660A voltammetric analyzer. A three-electrode system in a single-compartment cell with resistance compensation was used throughout. The working electrode was a glassy carbon disk (diameter = 3 mm). This electrode was carefully polished with 1, 0.3, and 0.05 μm alumina powder, respectively, and ultrasonically rinsed with distilled water and ethanol before each run. The auxiliary electrode was a platinum sheet, and the reference electrode was Ag/AgCl in CH_2Cl_2 with 0.1 M TBAP. The ferrocene/ferrocenium redox couple was located at 0.39 V under our experimental conditions.

[Ru(CHC(PPh₃)CHC(PPh₃)CH)Cl₂(PPh₃)₂Cl (2). A mixture of $[\text{RuCl}_2(\text{PPh}_3)_3]$ (0.60 g, 0.63 mmol), $\text{HC}\equiv\text{CCH}(\text{OH})\text{C}\equiv\text{CH}$ (55 mg, 0.69 mmol), PPh_3 (0.83 g, 3.2 mmol), and Bu_4NCl (0.40 g, 5.4 mmol) in THF (10 mL) was stirred at room temperature for about 10 h to give a brownish-green suspension. The green solid was collected by filtration, washed with THF (5×2 mL), and then dried under vacuum. Yield: 0.45 g, 55%. $^{31}\text{P}\{^1\text{H}\}$ NMR (121.5 MHz, CDCl_3): δ 18.2 (s, CPh_3), 8.1 (s, RuPh_3). ^1H NMR (300.1 MHz, CDCl_3): δ 17.5 (d, $J(\text{PH}) = 18.9$ Hz, 2 H, RuCH), 8.2 (t, $J(\text{PH}) = 14.0$ Hz, 1 H, $\text{RuCHC}(\text{PPh}_3)\text{CH}$), 7.9–6.6 (m, 60 H, PPh_3). $^{13}\text{C}\{^1\text{H}\}$ NMR (125.7 MHz, CD_2Cl_2): δ 284.3 (d, $J(\text{PC}) = 11.6$ Hz, RuCH), 146.0 (t, $J(\text{PC}) = 21.4$ Hz, $\text{RuCHC}(\text{PPh}_3)\text{CH}$), 137.3–126.8 (m, PPh_3), 108.3 (dd, $J(\text{PC}) = 73.2$ Hz, $J(\text{PC}) = 12.1$ Hz, $\text{RuCHC}(\text{PPh}_3)$). Anal. Calcd for $\text{C}_{77}\text{H}_{63}\text{Cl}_3\text{P}_4\text{Ru}$: C, 70.08; H, 4.81. Found: C, 69.65; H, 4.88.

[Ru(CHC(PPh₃)CHC(PPh₃)CH)Cl₂(PPh₃)₂BF₄ (2'). A mixture of $[\text{RuCl}_3 \cdot 3\text{H}_2\text{O}]$ (0.15 g, 0.57 mmol), PPh_3 (1.0 g, 4.0 mmol), and $\text{HC}\equiv\text{CCH}(\text{OH})\text{C}\equiv\text{CH}$ (51 mg, 0.63 mmol) in the mixed solution of $[\text{Bmim}]\text{BF}_4$ (0.5 mL) and CH_2Cl_2 (5 mL) was stirred at room temperature for ca. 7 h to give a brown solution. The solvent was evaporated to dryness under vacuum, and the resulting residue was washed with isopropyl alcohol (5×2 mL), ether (5×2 mL), and

(24) Jones, E. R. H.; Lee, H. H.; Whiting, M. C. *J. Chem. Soc.* **1960**, 3483.

Table 1. Crystal Data and Structure Refinement for 2, 4, 7, 8, 9, and 10

	2	4	7	8	9	10
empirical formula	C _{77.50} H ₇₁ Cl ₄ Ru- O _{3.50} P ₄	C ₄₇ H _{57.50} Cl ₃ Ru- O _{3.25} P ₄	C _{70.50} H ₆₅ Cl ₆ Ru- N ₂ O ₃ P ₃	C ₅₇ H ₅₉ Cl ₃ RuN ₂ P ₄	C ₁₁₈ H ₉₆ Cl ₃ Ru ₂ - B ₃ F ₁₂ O _{0.50} P ₆	C ₄₁ H ₃₃ ClP ₂
fw	1425.09	1005.73	1394.92	1103.36	2276.69	623.06
temperature, K	223(2)	223(2)	223(2)	223(2)	223(2)	223(2)
radiation (Mo K α), Å	0.71073	0.71073	0.71073	0.71073	0.71073	0.71073
cryst syst	monoclinic	monoclinic	triclinic	orthorhombic	triclinic	triclinic
space group	<i>P</i> 2 ₁ / <i>n</i>	<i>P</i> 2 ₁ / <i>c</i>	<i>P</i> 1	<i>F</i> ddd	<i>P</i> 1	<i>P</i> 1
<i>a</i> , Å	17.580(2)	11.776(3)	13.915(2)	24.495(4)	13.198(2)	9.4106(17)
<i>b</i> , Å	24.385(3)	20.801(6)	14.921(2)	25.713(4)	19.435(4)	10.611(2)
<i>c</i> , Å	18.446(3)	20.544(6)	18.165(3)	43.627(10)	21.924(4)	16.299(3)
α , deg	90	90	104.201(2)	90	80.074(3)	102.528(3)
β , deg	110.948(2)	105.677(5)	106.209(3)	90	89.858(3)	101.903(3)
γ , deg	90	90	102.962(3)	90	84.173(3)	95.411(3)
<i>V</i> , Å ³	7385.3(17)	4845(2)	3332.6(9)	27479(9)	5510.1(17)	1538.1(5)
<i>Z</i>	4	4	2	16	2	2
<i>d</i> _{calcd} , g cm ⁻³	1.282	1.379	1.390	1.067	1.372	1.345
abs coeff, mm ⁻¹	0.490	0.660	0.596	0.468	0.503	0.259
<i>F</i> (000)	2944	2082	1434	9120	2320	652
cryst size, mm	0.35 × 0.30 × 0.16	0.27 × 0.17 × 0.12	0.41 × 0.27 × 0.23	0.40 × 0.33 × 0.38	0.32 × 0.26 × 0.12	0.32 × 0.20 × 0.14
θ range, deg	1.67–25.00	1.42–26.00	1.24–25.50	1.81–26.00	0.94–25.00	1.99–26.00
no. of reflns collected	53 143	37 547	33 450	49 116	39 908	16 127
no. of indep reflns	12 954	9518	12 344	6461	19 200	6014
no. of obsd reflns (<i>I</i> > 2 σ (<i>I</i>))	10 129	8493	11 133	5151	14 998	5293
no. of data/restraints/ params	12 954/0/847	9518/0/532	12 344/0/784	6461/3/329	19 200/80/1278	6014/0/397
goodness-of-fit on <i>F</i> ²	1.085	1.173	1.153	1.103	1.132	1.123
final <i>R</i> (<i>I</i> > 2 σ (<i>I</i>))	<i>R</i> ₁ = 0.0757, <i>wR</i> ₂ = 0.1916	<i>R</i> ₁ = 0.0735, <i>wR</i> ₂ = 0.1491	<i>R</i> ₁ = 0.0699, <i>wR</i> ₂ = 0.1776	<i>R</i> ₁ = 0.0750, <i>wR</i> ₂ = 0.1867	<i>R</i> ₁ = 0.0869, <i>wR</i> ₂ = 0.2225	<i>R</i> ₁ = 0.0612, <i>wR</i> ₂ = 0.1471
<i>R</i> indices (all data)	<i>R</i> ₁ = 0.0970, <i>wR</i> ₂ = 0.2033	<i>R</i> ₁ = 0.0847, <i>wR</i> ₂ = 0.1546	<i>R</i> ₁ = 0.0773, <i>wR</i> ₂ = 0.1822	<i>R</i> ₁ = 0.0925, <i>wR</i> ₂ = 0.1970	<i>R</i> ₁ = 0.1081, <i>wR</i> ₂ = 0.2343	<i>R</i> ₁ = 0.0699, <i>wR</i> ₂ = 0.1522
peak and hole, e Å ⁻³	1.150 and -0.874	1.104 and -0.934	1.404 and -0.602	1.123 and -0.467	1.795 and -0.862	0.707 and -0.268

THF (3 × 2 mL) and dried under vacuum. Yield: 0.55 g, 70%. Anal. Calcd for C₇₇H₆₅Cl₂P₄BF₄Ru: C, 67.46; H, 4.63. Found: C, 67.49; H, 4.62.

[Ru(CHC(PPh₃)CHC(PPh₃)CH)Cl₂(PMe₃)₂]Cl (3). A solution of PMe₃ in THF (1.0 M; 4.5 mL, 4.5 mmol) was added to a solution of **2** (0.40 g, 0.31 mmol) in CH₂Cl₂ (10 mL). The reaction mixture was stirred at room temperature for about 12 h to give a brown solution. The volume of the mixture was reduced to approximately 1 mL under vacuum. The residue was purified by column chromatography (neutral alumina, eluent: acetone/methanol, 5:1) to give **3** as a green solid. Yield: 0.17 g, 58%. ³¹P{¹H} NMR (202.4 MHz, CDCl₃): δ 18.1 (s, CPh₃), -13.9 (s, RuPMe₃). ¹H NMR (500.4 MHz, CDCl₃): δ 17.0 (d, *J*(PH) = 16.5 Hz, 2 H, RuCH), 7.9 (t, *J*(PH) = 14.5 Hz, 1 H, RuCHC(PPh₃)CH), 7.8–7.2 (m, 30 H, PPh₃), 0.88 (t, *J*(PH) = 4.1 Hz, 18 H, RuPMe₃). ¹³C{¹H} NMR (125.7 MHz, CDCl₃): δ 279.6 (d, *J*(PC) = 12.7 Hz, RuCH), 143.3 (t, *J*(PC) = 23.0 Hz, RuCHC(PPh₃)CH), 134.9–128.4 (m, PPh₃), 107.3 (dd, *J*(PC) = 75.2 Hz, *J*(PC) = 12.0 Hz, RuCHC(PPh₃)), 15.7 (t, *J*(PC) = 15.4 Hz, PMe₃). Anal. Calcd for C₄₇H₅₁Cl₃P₄Ru: C, 59.60; H, 5.43. Found: C, 59.79; H, 4.96.

[Ru(CHC(PPh₃)CHC(PPh₃)CH)Cl₂(PBu₃)₂]Cl (5). PBu₃ (1.1 mL, 4.5 mmol) was added to a solution of **2** (0.40 g, 0.31 mmol) in CHCl₃ (10 mL). The reaction mixture was stirred at room temperature for ca. 0.5 h to give a green solution. The volume of the mixture was reduced to ca. 3 mL under vacuum. Addition of diethyl ether (20 mL) to the solution gave a brownish-green precipitate, which was collected by filtration, and subsequent recrystallization of the crude product from dichloromethane/ether yielded dark green crystals. Yield: 0.23 g, 65%. ³¹P{¹H} NMR (121.5 MHz, CDCl₃): δ 19.1 (s, CPh₃), 5.8 (s, RuPBu₃). ¹H NMR (300.1 MHz, CDCl₃): δ 17.6 (d, *J*(PH) = 17.7 Hz, 2 H, RuCH), 8.0 (t, *J*(PH) = 14.1 Hz, 1 H, RuCHC(PPh₃)CH), 7.9–7.3 (m, 30 H, PPh₃), 0.7–1.2 (m, 54 H, RuPBu₃). ¹³C{¹H} NMR (75.5 MHz, CDCl₃): δ 278.3 (d, *J*(PC) = 11.2 Hz, RuCH), 143.9 (t, *J*(PC) = 21.2 Hz, RuCHC(PPh₃)CH), 135.4–130.4 (m, PPh₃), 105.0 (dd,

J(PC) = 72.5 Hz, *J*(PC) = 13.2 Hz, RuCHC(PPh₃)) 25.3–13.8 (m, PBu₃). Anal. Calcd for C₆₅H₈₇P₄Cl₃Ru: C, 65.07; H, 7.31. Found: C, 64.98; H, 7.07.

[Ru(CHC(PPh₃)CHC(PPh₃)CH)Cl(*t*-BuNC)(PPh₃)₂]Cl₂ (6). *t*-BuNC (0.53 mL, 4.5 mmol) was added to a solution of **2** (0.40 g, 0.31 mmol) in CH₂Cl₂ (10 mL). The reaction mixture was stirred at room temperature for about 1 h to give a brown solution. The volume of the mixture was reduced to approximately 1 mL under vacuum. The residue was purified by column chromatography (neutral alumina, eluent: acetone/methanol, 5:1) to give **5** as a green solid. ³¹P{¹H} NMR (202.4 MHz, CDCl₃): δ 25.1 (s, RuPPh₃), 23.3 (s, CPh₃), 18.3 (s, CPh₃). ¹H NMR (500.4 MHz, CDCl₃): δ 15.6 (d, *J*(PH) = 23.3 Hz, 1 H, RuCH), 15.5 (d, *J*(PH) = 19.0 Hz, 1 H, RuCH), 8.0 (t, *J*(PH) = 13.5 Hz, 1 H, RuCHC(PPh₃)CH), 7.8–6.7 (m, 60 H, PPh₃), 1.1 (s, 9 H, (CH₃)₃CNC). ¹³C{¹H} NMR (125.7 MHz, CD₂Cl₂): δ 286.1 (d, *J*(PC) = 9.8 Hz, RuCH), 280.6 (d, *J*(PC) = 10.2 Hz, RuCH), 149.1 (t, *J*(PC) = 22.1, RuCHC(PPh₃)CH), 136.3–128.4 (m, PPh₃), 123.3 (s, (CH₃)₃CNC), 113.7 (d, *J*(PC) = 72.3 Hz, RuCHC(PPh₃)), 113.6 (d, *J*(PC) = 72.8 Hz, RuCHC(PPh₃)), 58.7 (s, (CH₃)₃CNC), 29.2 (s, (CH₃)₃CNC). Anal. Calcd for C₈₂H₇₂NP₄Cl₃Ru: N, 1.00; C, 70.21; H, 5.17. Found: N, 1.35; C, 70.24; H, 5.51.

[Ru(CHC(PPh₃)CHC(PPh₃)CH)Cl(bipy)(PPh₃)Cl₂ (7). 2,2'-Dipyridyl (94 mg, 0.60 mmol) was added to a solution of **2** (0.40 g, 0.31 mmol) in CH₂Cl₂ (10 mL). The reaction mixture was stirred at room temperature for about 5 h to give a brown-green solution. The volume of the mixture was reduced to approximately 1 mL under vacuum. The residue was purified by column chromatography (neutral alumina, eluent: acetone/methanol, 5:1) to give **7** as a green solid. Yield: 0.21 g, 49%. ³¹P{¹H} NMR (202.4 MHz, CDCl₃): δ 45.6 (t, *J*(PP) = 2.6 Hz, RuPPh₃), 19.0 (d, *J*(PP) = 2.6 Hz, CPh₃). ¹H NMR (500.4 MHz, CDCl₃): δ 15.6 (dd, *J*(PH) = 16.0 Hz, *J*(PH) = 8.0 Hz, 2 H, RuCH), 9.0 (d, *J*(HH) = 8.0 Hz, 2 H, NCH), 8.2 (t, *J*(PH) = 8.0 Hz, 1 H, RuCHC(PPh₃)CH), 7.8–6.7 (m, 51 H, PPh₃, 2,2'-dipyridyl). ¹³C{¹H} NMR (125.7 MHz, CD₂Cl₂): δ 293.6

(d, $J(\text{PC}) = 12.6$ Hz, RuCH), 147.7 (t, $J(\text{PC}) = 22.8$ Hz, RuCHC(PPh₃)CH), 154.0, 147.5, 140.0, 126.0, 124.9 (s, N(CH₂)₄CC(CH₂)₄N), 136.3–128.4 (m, PPh₃), 120.2 (dd, $J(\text{PC}) = 75.8$ Hz, $J(\text{PC}) = 13.1$ Hz, RuCHC(PPh₃)). Anal. Calcd for C₆₉H₅₆N₂P₃Cl₃Ru: N, 2.31; C, 68.29; H, 4.65. Found: N, 2.06; C, 68.13; H, 4.87.

[Ru(CHC(PPh₃)CHC(PPh₃)CH)(bipy)(PMe₃)₂]Cl₃ (8). A solution of PMe₃ in THF (1.0 M; 4.9 mL, 4.9 mmol) was added to a solution of **7** (0.40 g, 0.33 mmol) in CH₂Cl₂ (10 mL). The reaction mixture was stirred at room temperature for ca. 24 h to give a brownish-green suspension. The green solid was collected by filtration, washed with THF (3 × 2 mL), and then dried under vacuum. Yield: 0.15 g, 40%. ³¹P{¹H} NMR (121.5 MHz, CDCl₃): δ 19.6 (s, CPPh₃), -12.1 (s, RuPMe₃). ¹H NMR (300.1 MHz CD₃OD): δ 16.1 (dd, $J(\text{PH}) = 17.7$ Hz, $J(\text{PH}) = 2.4$ Hz, 2 H, RuCH), 8.0 (t, $J(\text{PH}) = 15.0$ Hz, 1 H, RuCHC(PPh₃)CH), 7.6–9.4 (m, 53 H, PPh₃, 2,2'-dipyridyl), 1.63 (t, $J(\text{PH}) = 4.1$ Hz, 18 H, RuPMe₃). ¹³C{¹H} NMR (75.5 MHz, CD₃OD): δ 291.0 (dd, $J(\text{PC}) = 11.4$ Hz, $J(\text{PC}) = 11.4$ Hz, RuCH), 149.6 (t, $J(\text{PC}) = 21.5$ Hz, RuCHC(PPh₃)CH), 154.2, 149.8, 141.3, 128.0, 125.4 (s, N(CH₂)₄CC(CH₂)₄N), 135.5–130.6 (m, PPh₃), 114.5 (dd, $J(\text{PC}) = 75.2$ Hz, $J(\text{PC}) = 12.1$ Hz, RuCHC(PPh₃)), 12.5 (t, $J(\text{PC}) = 15.9$ Hz, PMe₃). Anal. Calcd for C₅₇H₅₉N₂P₄Cl₃Ru: N, 2.54; C, 62.04; H, 5.39. Found: N, 2.14; C, 62.17; H, 4.98.

[Ru(CHC(PPh₃)CHC(PPh₃)CH)(PPh₃)₂(μ-Cl)₃(BF₄)₃ (9). A mixture of **2** (0.80 g, 0.62 mmol) and AgBF₄ (0.25 g, 1.24 mmol) in CH₂Cl₂ (20 mL) was stirred at room temperature for ca. 6 h to give a green suspension. The white-silver salt was removed by filtration, while the green filtrate was collected and reduced to ca. 2 mL under vacuum. Addition of ether (10 mL) to recrystallize the crude product yielded green crystals. Yield: 0.52 g, 74%. ³¹P{¹H} NMR (121.5 MHz, CD₂Cl₂): δ 34.6 (s, RuPPh₃), 20.1 (s, CPPh₃), 18.8 (s, CPPh₃). ¹H NMR (300.1 MHz, CD₂Cl₂): δ 16.1 (d, $J(\text{PH}) = 14.7$ Hz, 2 H, RuCH), 16.0 (d, $J(\text{PH}) = 14.4$ Hz, 2 H, RuCH), 7.6–6.8 (m, 90 H, PPh₃). ¹³C{¹H} NMR (75.5 MHz, CD₂Cl₂): δ 292.3 (d, $J(\text{PC}) = 11.3$ Hz, RuCH), 289.1 (d, $J(\text{PC}) = 12.8$ Hz, RuCH), 145.5 (t, $J(\text{PC}) = 21.5$, RuCHC(PPh₃)CH), 135.2–128.0 (m, PPh₃), 117.2 (dd, $J(\text{PC}) = 75.0$ Hz, $J(\text{PC}) = 13.3$ Hz, RuCHC(PPh₃)), 115.98 (dd, $J(\text{PC}) = 75.0$ Hz, $J(\text{PC}) = 13.3$ Hz, RuCHC(PPh₃)). Anal. Calcd for C₁₁₈H₉₆P₆Cl₃Ru₂B₃F₁₂: C, 62.47; H, 4.26. Found: C, 62.84; H, 4.52.

[CHC(PPh₃)CHC(PPh₃)CH]Cl (10). Method A: A solid sample of **2** (0.40 g, 0.31 mmol) was heated at 150 °C for 5 h. The mixture

was solved in 5 mL of CH₂Cl₂ to give a brown solution. The mixture was purified by column chromatography (neutral alumina, eluent: acetone/CH₂Cl₂ mixture, 1:2) to give **10** as a light yellow solid. Yield: 0.17 g, 90%. Method B: A solid sample of **7** (0.40 g, 0.33 mmol) was heated at 100 °C for 2 h. The mixture was solved in 5 mL of CH₂Cl₂ to give a brown solution. The mixture was purified by column chromatography (neutral alumina, eluent: acetone/CH₂Cl₂ mixture, 1:2) to give **10** as a light yellow solid. Yield: 0.17 g, 85%. ³¹P{¹H} NMR (121.5 MHz, CDCl₃): δ 14.2 (s; CPPh₃). ¹H NMR (300.1 MHz, CDCl₃): δ 7.8–7.5 (m, 30 H; PPh₃), 6.6 (m, 2 H; CHC(PPh₃)CHC(PPh₃)), 6.2 (m, 1 H; C(PPh₃)-CHC(PPh₃)). ¹³C{¹H} NMR (75.5 MHz, CDCl₃): δ 134.1–129.3 (m, PPh₃), 122.9 (d, $J(\text{PC}) = 91.4$ Hz, CHC(PPh₃)), 121.1 (t, $J(\text{PC}) = 15.9$ Hz, C(PPh₃)CHC(PPh₃)), 92.8 (dd, $J(\text{PC}) = 109.5$ Hz, $J(\text{PC}) = 17.7$ Hz, C(PPh₃)). Anal. Calcd for C₄₁H₃₃ClP₂: C, 79.03; H, 5.34. Found: C, 79.21; H, 5.52.

Crystallographic Analysis. Crystals suitable for X-ray diffraction were grown from CH₂Cl₂ or CH₃OH solutions layered with ether for **2**, **4**, **7**, **8**, **9**, and **10**. Selected crystals of **2**, **4**, **7**, **8**, **9**, and **10** were mounted on top of a glass fiber and transferred into a cold stream of nitrogen. Data collections were performed on a Bruker Apex CCD area detector using graphite-monochromated Mo K α radiation ($\lambda = 0.71073$ Å). Multiscan absorption corrections (SADABS) were applied. All structures were solved by direct methods, expanded by difference Fourier syntheses, and refined by full-matrix least-squares on F^2 using the Bruker SHELXTL (Version 6.10) program package. Non-H atoms were refined anisotropically unless otherwise stated. Hydrogen atoms were introduced at their geometric positions and refined as riding atoms. Further details on crystal data, data collection, and refinements are summarized in Table 1.

Acknowledgment. This work was supported by the program New Century Excellent Talents in Universities of China (NCET-04-0603) and the National Science Foundation of China (20572089).

Supporting Information Available: X-ray crystallographic files (CIF). This material is available free of charge via the Internet at <http://pubs.acs.org>.

OM070195K